sidering the M–N bond strength in the $M(HDMG)_2$ complexes; they are reported[20] to decrease in the order Pt(II) > Pd(II) > Cu(II) > Ni(II). The higher Cu–N bond strength presumably more than compensates for the strain in the five-membered rings of the $Cu(\beta\text{-}HCQD)_2\cdot H_2O\cdot{}^1/_2$dioxane.

In the complexes $Pd(\beta\text{-}H_2CQD)Cl_2$, $Pt(\beta\text{-}H_2CQD)Cl_2$, and $Cu(\beta\text{-}H_2CQD)Cl_2$, the neutral $\beta\text{-}H_2CQD$ ligand also chelates through both N atoms. This type of compound exhibits a strong infrared absorption for coordinated $\nu(C{=}N)$ between 1450 and 1400 cm^{-1}.

In the complexes $Pd(\gamma\text{-}H_2CQD)_2Cl_2$, $Pd(\delta\text{-}H_2CQD)_2Cl_2$, and $Pd(\alpha\text{-}H_2CQD)_2Cl_2$, the H_2CQD ligand coordinates through only one of its N atoms. Since our attempts to synthesize similar Pd complexes from H_2DMG and H_2CHD were unsuccessful, the $Pd(H_2CQD)_2Cl_2$ complexes are the first reported examples of a monodentate α-dioxime ligand. This type of complex is probably stabilized to some extent by the formation of inter- or intramolecular H bonds as in the case of bis(cyclohexanone oxime)palladium dichloride.[30] Finally, in $[Pt(\gamma\text{-}HCQD)(\gamma\text{-}H_2CQD)Cl]_2$ and $Ni(\delta\text{-}HCQD)_2(\delta\text{-}H_2CQD)_2$, the ligands also appear to coordinate as monodentate ligands but in the unusual proposed structures shown in Figures 8 and 12.

Acknowledgment. We appreciate the support of this research by the National Institute of General Medical Sciences (Grant No. GM12626).

Registry No. $Ni(\delta\text{-}HCQD)_2$, 52139-64-7; $Ni(\alpha\text{-}HCQD)_2$, 52231-70-6; $Ni(\delta\text{-}HCQD)_2(\delta\text{-}H_2CQD)_2$, 72100-32-4; $Cu(\beta\text{-}HCQD)_2$, 72100-33-5; $Cu(\beta\text{-}H_2CQD)Cl_2$, 72100-34-6; $Pd(\beta\text{-}HCQD)_2$, 71212-51-6; $Pd(\delta\text{-}HCQD)_2$, 72100-35-7; $Pt(\beta\text{-}HCQD)_2$, 72100-36-8; $Pd(\gamma\text{-}H_2CQD)_2Cl_2$, 72100-37-9; $Pd(\delta\text{-}H_2CQD)_2Cl_2$, 72121-18-7; $Pd(\alpha\text{-}H_2CQD)_2Cl_2$, 72150-72-2; $Pd(\beta\text{-}H_2CQD)Cl_2$, 72100-38-0; $Pt(\beta\text{-}H_2CQD)Cl_2$, 72100-39-1; $Pd(H_2CHD)Cl_2$, 72100-40-4; $Pd(H_2DMG)Cl_2$, 30184-40-8; $[Pt(\gamma\text{-}HCQD)(\gamma\text{-}H_2CQD)Cl]_2$, 72121-19-8.

---

(30) Tanimura, M.; Mizushima, T.; Kinoshita, Y. *Bull. Chem. Soc. Jpn.* **1967**, *40*, 2777.

Contribution from the Chemistry Division, Argonne National Laboratory, Argonne, Illinois 60439,
and the Chemistry Department, University of California, Berkeley, California 94720

Coordinately Unsaturated Metal Clusters. A Neutron Diffraction Study of the Crystal and Molecular Structure of the Trimeric Rhodium Complex $\{HRh[P(OCH_3)_3]_2\}_3$[1]

RICHARD K. BROWN,[2a] JACK M. WILLIAMS,*[2a] ANDREW J. SIVAK,[2b] and EARL L. MUETTERTIES*[2b]

Received July 26, 1979

The molecular structure of $\{HRh[P(OCH_3)_3]_2\}_3$ has been determined by using neutron diffraction techniques [T = 110 K]. The trimeric rhodium complex is monoclinic, space group $P2_1$ [$C_2{}^2$, No. 4], with a = 10.792 (6) Å, b = 13.438 (8) Å, c = 13.438 (8) Å, β = 91.64 (4)°, V_c = 1948.02 Å^3, and d_{calcd} = 1.801 g cm^{-3} for Z = 2. The neutral molecule consists of a triangular array of Rh atoms each bonded in an approximately square-planar fashion to two terminal $P(OCH_3)_3$ groups and two bridging hydride ligands. The Rh–Rh separations involving single hydrogen bridges are 2.803 (7), 2.780 (6), and 2.856 (8) Å and the average Rh–H_b distance is 1.76 (3) Å. The bridging Rh–H_b separations reported here are the first interactions to be characterized structurally with neutron crystallographic techniques (T = 110 K). A discussion of the origin of the structural distortion from planarity of the $\{HRhP_2\}_3$ cluster core is presented.

Introduction

The di- and trimeric rhodium clusters $\{HRh[P(O\text{-}i\text{-}C_3H_7)_3]_2\}_2$ (**1**) and $\{HRh[P(OCH_3)_3]_2\}_3$ (**2**) have recently been shown to be exceedingly active catalysts toward the hydrogenation of olefins.[3,4] These two clusters, the smallest oligomers for a potentially large set of hydrides of the form $\{HRh[P(OR)_3]_2\}_x$, have been shown to reversibly and rapidly add 1 molecule of hydrogen/molecule of cluster without detectable fragmentation of the cluster. The fact that the clusters themselves, rather than mononuclear $H_3Rh[P(OR)_3]_2$ fragments, are the principal intermediates in the catalytic hydrogenation of olefins suggests that these clusters, their hydrogen adducts, and the hydrogen adduct–olefin complexes[4] may be viewed as tentative models of intermediates in olefin hydrogenation on metal surfaces.[6–13] Accordingly, the precise structural and stereochemical features of these polynuclear rhodium species are of considerable interest especially since the detailed structural characterization, at the molecular level, of hydrocarbon substrates chemisorbed on metal surfaces is an exceedingly difficult task.[12] The isolation of large single crystals of complexes **1** and **2** has allowed structural characterization of these potential catalytic surface–substrate models.[4,12,13] We report here the complete neutron diffraction structural characterization of **2**. Although the nonhydrogen atom framework was previously determined by X-ray diffraction,[3] the complete structural characterization of the $\{HRhP_2\}_3$ core required neutron diffraction analysis. A preliminary account of this work has been previously reported.[4]

Experimental Section

The trimeric rhodium complex, **2**, is monoclinic space group $P2_1$ [$C_2{}^2$, No. 4] with a = 10.792 (6) Å, b = 13.438 (8) Å, c = 13.438

---

(1) This work was performed under the auspices of the Office of Basic Energy Sciences of the United States Department of Energy. We also wish to acknowledge the partial support of this collaborative research by the National Science Foundation (Grant No. CHE-78-20698) through a grant to J.M.W. and E.L.M.

(2) (a) Argonne National Laboratory. (b) University of California at Berkeley.

(3) Day, V. W.; Fredrich, M. F.; Reddy, G. S.; Sivak, A. J.; Pretzer, W. R.; Muetterties E. L. *J. Am. Chem. Soc.* **1977**, *99*, 8091.

(4) (a) Brown, R. K.; Williams, J. M.; Fredrich, M. F.; Day, V. W.; Sivak, A. J.; Muetterties, E. L. *Proc. Natl. Acad. Sci. U.S.A.* **1979**, *76*, 2099. (b) Sivak, A. J.; Muetterties, E. L. *J. Am. Chem. Soc.* **1979**, *101*, 4878.

(5) Strouse, C. E. *Rev. Sci. Instrum.* **1976**, *47*, 871.

(6) Burwell, R. L., Jr. *Chem. Eng. News* **1966**, *44* (34), 56.

(7) Ugo, R. *Catal. Rev.* **1975**, *11*, 225.

(8) Lewis, J.; Johnson, B. F. G. *Pure Appl. Chem.* **1975**, *44*, 43.

(9) Muetterties, E. L. *Science* **1977**, *196*, 839.

(10) Muetterties, E. L. *Bull. Soc. Chim. Belg.* **1975**, *84*, 959.

(11) Muetterties, E. L. *Bull. Soc. Chim. Belg.* **1976**, *85*, 451.

(12) Muetterties, E. L. *Angew. Chem., Int. Ed. Engl.* **1978**, *17*, 545.

(13) Muetterties, E. L.; Rhodin, T.; Band, E.; Brucker, C.; Pretzer, W. R. *Chem. Rev.* **1979**, *79*, 91.

0020-1669/80/1319-0370$01.00/0

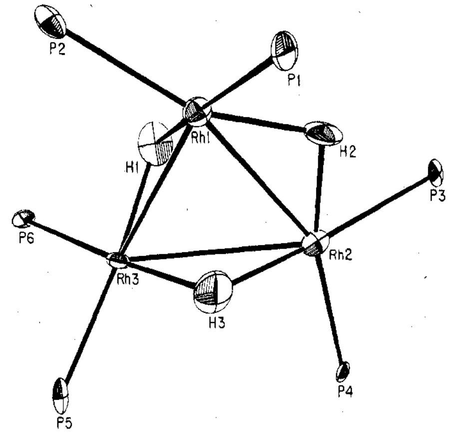

Figure 1. The inner core ($Rh_3H_3P_6$) of the $\{HRh[P(OCH_3)_3]_2\}_3$ molecular structure. Note the pseudo(noncrystallographic)-two-fold axis about a vector through Rh(3) and H(2). The thermal ellipsoids of nuclear motion for all atoms are scaled to enclose 50% probability.

(8) Å, $\beta = 91.64$ (4)°, $V_c = 1948.02$ Å^3, and $d_{calcd} = 1.801$ g cm^{-3} at 110 K for $Z = 2$. Full details of the single-crystal preparation are given elsewhere.[4] A large single crystal of $\{HRh[P(OCH_3)_3]_2\}_3$, weighing 55 mg, was sealed under dry N_2 in a Pb glass capillary for protection. A total of 3186 independent three-dimensional data, of which 2698 had $F_o^2 > \sigma(F_o^2)$, were collected by using an Electronics and Alloys four-circle diffractometer at the Argonne CP-5 reactor. All data were collected at 110 K, using a device based on the Strouse design,[5] out to $((\sin\theta)/\lambda = 0.577$ Å^{-1} (λ 1.142 (1) Å)). The cell constants and crystal orientation were determined from a least-squares fit of 21 automatically centered reflections with $40° < 2\theta < 50°$. All data were collected by using a θ–2θ step scan and integrated intensities were corrected for absorption ($\mu_c = 2.38$ cm^{-1}), the range of transmission coefficients being 0.354–0.505. By use of initial nonhydrogen atom coordinates from the room-temperature X-ray investigation, all atoms were located by using Fourier techniques. Final anisotropic full-matrix least-squares refinement of all 102 atoms (919 parameters) on the Argonne IBM 370/195 computer gave $R(F_o^2) = 0.117$ and $R(F_o) = 0.101$ with a "goodness of fit" of 1.42 for all data and $R(F_o^2) = 0.106$ and $R_w(F_o) = 0.072$ for data with $F_o^2 > \sigma(F_o^2)$. The function minimized was $\sum w_i(F_o^2 - F_c^2)^2$ with $w_i^{-1} = \sigma^2(F_o^2) = \sigma_c^2(F_o^2) + (0.05F_o^2)^2$ where σ_c is determined by counting statistics. The constant 0.05 used in the weighting scheme represents the 5% maximum variation observed in the integrated intensities of the two reference reflections used during data collection. Final Fourier difference density maps were essentially featureless. Final positional and thermal parameters are presented in Table I. For the least-squares refinement the coherent neutron scattering amplitudes (in units of 10^{-12} cm) used for Rh, C, O, P, and H were 0.58, 0.665, 0.580, 0.51, and −0.374, respectively.

Results and Discussion

Interatomic distances and angles for **2** are presented in Table II. The numbering scheme used to identify the inner core of the cluster is shown in Figure 1 and a stereoscopic view of the molecule is presented in Figure 2. The crystal structure consists of discrete and well-separated neutral trimeric molecules with the crystal packing dominated primarily by the bulky trimethyl phosphite ligands. The nonbonded inter- and intramolecular contacts are of the order of van der Waals distances or greater. The intermolecular interactions with distances less than 2.50 Å are listed in Table III.

Although the triangular rhodium cluster possesses no inherent crystallographic symmetry, it does have approximate C_2 symmetry with the pseudo-twofold axis passing through Rh(3) and H(2). Each rhodium atom is bonded in an approximately square-planar fashion to two terminal $P(OCH_3)_3$ groups and two bridging hydride ligands (H_b). The Rh–Rh separations of 2.803 (7) Å, 2.780 (6) Å, and 2.856 (8) Å arise from three Rh–H–Rh two-electron three-center (2e-3c) bonds. These separations are significantly longer than the Rh–Rh distance of 2.650 (2) Å found for **1** which arises from two

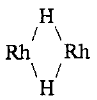

two-electron four-center (2e-4c) bonding interactions.[4] Although the rhodium–rhodium separation in the bulk metal[14] is 2.69 Å, normal two-electron (2e-2c) Rh–Rh bonds are generally in the range of 2.62–2.80 Å.[15,16,17] As expected, the (2e-3c) Rh–Rh separations in **2** are somewhat longer than the normal range of Rh–Rh separations found in clusters in which there is no bridging atom or group. The average Rh–H_b distance of 1.76 (3) Å for **2** is slightly longer than the approximate sum of the covalent radii, 1.72 Å.

Although numerous transition-metal hydrides have been studied by using X-ray diffraction techniques, only a limited number has been investigated by using neutron diffraction. Because this is the first neutron crystallographic study of a rhodium hydride complex, there are no other reliable Rh–H distances with which to compare those of **2** except for values determined from X-ray diffraction data. The average Rh–H_b distance in **2** is 1.76 Å which is similar to the values of 1.76 (6) Å and 1.78 (6) Å found by X-ray diffraction for the Rh–H_b separation in two Rh–H–B bonds.[18] Also, the average bridging Rh–H_b separation found in **2** is similar to the average values of 1.793 (4) and 1.862 (8) Å for the bridging M–H_b separations as determined by neutron diffraction studies of $(\mu_2\text{-H})Ru_3(CO)_9(C{\equiv}CCMe_3)$[19] and $Mo_2(\eta^5\text{-}C_5H_5)_2(CO)_4(\mu_2\text{-H})(\mu_2\text{-P(CH}_3)_2)$,[20] respectively. These data for second-row transition-metal bridging M–H_b distances show the expected slight increase in going from right to left in the periodic table.

The salient structural issue is the configuration of the $\{HRhP_2\}_3$ core. It is important to fully understand the structural, stereochemical and electronic features of this coordinately unsaturated cluster which does have the reactivity, in fact an extraordinary reactivity,[4b] hoped for in unsaturated metal clusters. Each RhH_2P_2 coordination unit is approximately "square" planar; thus there are three reactive metal sites in the cluster. Interestingly, the three square-planar RhH_2P_2 units are not coplanar with the Rh_3 triangle; the dihedral angles between the Rh_3 triangle and the square planes centered at Rh(1), Rh(2), and Rh(3) are not only nonzero but also vary substantially with angles of 35.1, 37.7, and 64.3°, respectively. As a result of this canting of the RhH_2P_2 units relative to the Rh_3 plane, H(1) and H(3) are displaced in opposite directions from the Rh_3 plane by 1.13 (2) and 1.03 (2) Å, respectively. In addition H(2) is displaced in the same direction as H(1) but by only 0.20 (2) Å. Although the relatively large estimated standard deviations associated with the Rh–H distances of **2** preclude any quantitative comparison of the nature of the Rh–H–Rh three-center bonds, it does

---

(14) Donahue, J. "The Structure of the Elements"; Wiley: New York, 1974; p 215.

(15) (a) Mills, O. S.; Nice J. P. *J. Organomet. Chem.* **1967**, *10*, 337. (b) Mills, O. S.; Paulus E. F. *ibid.* **1967**, *10*, 331. (c) Paulus, E. F. *Acta Crystallogr., Sect. B* **1969**, *25*, 2206. (d) Wei, C. H. *Inorg. Chem.* **1969**, *8*, 2384. (e) Dickson, R. S.; Johnson, S. H.; Kirsch, H. P.; Lloyd, D. J. *Acta Crystallogr., Sect. B* **1977**, *33*, 2057. (f) Herrmann, W. A.; Kruger, C.; Goddard, R.; Bernal, I. *Angew. Chem., Int. Ed. Engl.* **1977**, *16*, 334. (g) Cowie, M.; Mague, J. T.; Sanger, A. R. *J. Am. Chem. Soc.* **1978**, *100*, 3628.

(16) For example the Rh^I–Rh^I separation in $[(\eta^5\text{-}C_5H_5)_2Rh_2(CO)_3]$ is 2.68 Å.[15a] Rh^{III}–Rh^{III} separations are significantly longer (cf. Rh^{III}–Rh^{III} = 2.906 (1) Å in $[(\mu\text{-H})(\mu\text{-Cl})\{\eta^5\text{-}C_5(CH_3)_5RhCl\}_2]$.[17]

(17) Churchill, M. R.; Ni, S. W.-Y. *J. Am. Chem. Soc.* **1973**, *95*, 2150.

(18) Baker, R. T.; King, R. E., III; Knobler, C.; O'Con, C. A.; Hawthrone, M. F. *J. Am. Chem. Soc.* **1978**, *100*, 8266.

(19) Catti, M.; Gevasio, G.; Mason, S. A. *J. Chem. Soc., Dalton Trans.* **1978**, 2260.

(20) Petersen, J. L.; Dahl, L. F.; Williams, J. M. *J. Am. Chem. Soc.* **1974**, *96*, 6610.

Table I. Positional and Thermal Parameters (Å^2) for $\{HRh[P(OCH_3)_3]_2\}_3$[a]

ATOM	X	Y	Z	U11	U22	U33	U12	U13	U23
RH1	0.7398(5)	0.2700	0.4040(4)	0.007(2)	0.011(3)	0.010(2)	-0.001(2)	-0.006(2)	0.004(2)
RH2	0.7945(5)	0.3143(4)	0.2063(3)	0.013(2)	0.011(3)	0.003(2)	0.001(2)	0.003(2)	-0.003(2)
RH3	0.6336(5)	0.1535(4)	0.2535(4)	0.009(2)	0.007(3)	0.010(3)	-0.000(2)	-0.001(2)	-0.005(2)
H1	0.6012(9)	0.2607(8)	0.3218(8)	0.018(4)	0.026(6)	0.036(6)	0.010(4)	-0.013(4)	0.004(5)
H2	0.8063(10)	0.3578(8)	0.3275(7)	0.037(5)	0.025(5)	0.019(5)	-0.009(5)	-0.001(4)	0.001(4)
H3	0.7920(9)	0.1898(9)	0.2450(10)	0.017(5)	0.032(6)	0.069(8)	0.004(4)	0.011(5)	0.008(6)
P1	0.9043(5)	0.3026(5)	0.4927(5)	0.004(3)	0.024(4)	0.021(3)	-0.003(2)	-0.004(2)	-0.004(3)
O11	1.0314(5)	0.3270(5)	0.4359(5)	0.008(3)	0.032(4)	0.028(3)	-0.006(3)	0.000(2)	-0.001(3)
C11	1.0726(6)	0.2638(6)	0.3580(5)	0.021(3)	0.033(4)	0.031(3)	0.007(3)	0.005(3)	0.000(3)
H111	1.1590(14)	0.2904(16)	0.3373(12)	0.033(7)	0.121(16)	0.066(9)	-0.019(9)	0.024(7)	-0.029(10)
H112	1.0080(14)	0.2698(13)	0.2918(11)	0.043(7)	0.069(10)	0.058(9)	0.017(7)	0.006(7)	0.009(8)
H113	1.0831(22)	0.1912(15)	0.3845(14)	0.138(17)	0.051(12)	0.065(11)	0.029(11)	0.057(11)	0.004(9)
O12	0.9474(6)	0.2175(5)	0.5698(4)	0.017(3)	0.021(3)	0.025(3)	-0.001(3)	-0.004(2)	0.004(3)
C12	1.0538(6)	0.2262(6)	0.6335(5)	0.018(3)	0.031(4)	0.035(4)	0.001(3)	-0.010(3)	0.001(4)
H121	1.0354(15)	0.2760(15)	0.6903(13)	0.063(9)	0.078(12)	0.051(9)	0.013(9)	-0.004(7)	-0.018(10)
H122	1.1301(15)	0.2557(17)	0.5994(12)	0.035(7)	0.136(17)	0.061(9)	-0.018(9)	-0.015(7)	0.043(11)
H123	1.0728(15)	0.1531(13)	0.6603(14)	0.057(9)	0.041(9)	0.115(14)	-0.015(8)	-0.050(9)	0.016(10)
C13	0.9082(5)	0.3976(5)	0.5658(5)	0.015(3)	0.020(3)	0.026(3)	-0.002(2)	-0.002(2)	-0.004(3)
C13	0.8842(5)	0.4932(4)	0.5220(4)	0.013(2)	0.016(3)	0.032(3)	-0.000(2)	-0.001(2)	-0.001(3)
H131	0.8425(15)	0.5424(11)	0.5794(12)	0.071(9)	0.026(7)	0.075(10)	0.002(7)	0.023(8)	-0.010(7)
H132	0.9693(14)	0.5292(11)	0.5008(13)	0.052(8)	0.035(8)	0.096(11)	-0.019(7)	0.016(8)	0.000(8)
H133	0.8231(12)	0.4865(9)	0.4546(11)	0.043(7)	0.023(6)	0.067(8)	0.006(6)	-0.025(6)	-0.005(6)
P2	0.6492(5)	0.2049(5)	0.5331(4)	0.008(3)	0.016(3)	0.012(3)	-0.005(2)	-0.004(2)	-0.004(3)
O21	0.6860(6)	0.2627(5)	0.6338(4)	0.022(3)	0.022(3)	0.015(3)	-0.008(3)	-0.007(2)	-0.007(3)
C21	0.6627(7)	0.2225(7)	0.7290(4)	0.031(3)	0.066(5)	0.005(3)	-0.022(4)	0.002(2)	-0.005(4)
H211	0.6558(29)	0.2843(18)	0.7748(14)	0.227(28)	0.139(18)	0.049(10)	-0.112(20)	0.075(14)	-0.053(12)
H212	0.5795(17)	0.1852(17)	0.7340(10)	0.072(10)	0.155(20)	0.037(8)	-0.090(13)	-0.020(7)	0.041(10)
H213	0.7277(25)	0.1757(23)	0.7499(18)	0.102(16)	0.152(26)	0.086(16)	0.053(18)	0.009(12)	0.052(16)
O22	0.4993(5)	0.2029(5)	0.5353(4)	0.008(2)	0.027(4)	0.024(3)	-0.003(2)	0.001(2)	0.004(3)
C22	0.4268(5)	0.2846(5)	0.5003(5)	0.012(3)	0.028(3)	0.038(3)	-0.004(3)	0.001(2)	-0.007(3)
H221	0.4100(14)	0.3380(9)	0.5575(12)	0.071(9)	0.014(6)	0.063(9)	0.019(6)	0.002(7)	0.002(7)
H222	0.3394(15)	0.2543(13)	0.4788(16)	0.035(7)	0.050(9)	0.162(18)	0.001(7)	-0.051(10)	-0.009(11)
H223	0.4693(19)	0.3255(15)	0.4442(15)	0.091(12)	0.072(11)	0.105(14)	0.066(10)	0.066(12)	0.061(12)
O23	0.6627(6)	0.0909(5)	0.5638(5)	0.027(3)	0.029(3)	0.029(3)	-0.002(3)	0.012(3)	0.004(3)
C23	0.7591(6)	0.0300(6)	0.5311(6)	0.027(3)	0.018(4)	0.069(5)	0.005(3)	0.013(3)	0.007(4)
H231	0.8147(22)	0.0664(15)	0.4814(19)	0.113(15)	0.057(11)	0.153(21)	0.004(11)	0.096(17)	0.021(13)
H232	0.7335(21)	-0.0383(16)	0.5248(29)	0.076(13)	0.035(12)	0.289(40)	-0.002(10)	0.040(18)	-0.020(16)
H233	0.8342(20)	0.0312(20)	0.5972(22)	0.070(12)	0.106(18)	0.200(25)	0.014(13)	-0.086(16)	0.003(19)
P3	0.8005(5)	0.4730(5)	0.1795(5)	0.007(3)	0.012(3)	0.025(3)	0.002(2)	0.004(2)	-0.004(3)
O31	0.7275(6)	0.5096(4)	0.0785(4)	0.025(3)	0.039(3)	0.023(3)	0.006(2)	-0.001(2)	-0.001(3)
C31	0.7079(6)	0.6139(5)	0.0597(5)	0.019(3)	0.018(3)	0.030(3)	0.002(3)	0.001(3)	0.001(3)
H311	0.6328(15)	0.6393(10)	0.0980(11)	0.059(8)	0.032(7)	0.061(8)	0.036(7)	-0.005(8)	0.006(7)
H312	0.7917(14)	0.6551(10)	0.0730(14)	0.047(8)	0.024(7)	0.112(13)	-0.013(7)	-0.013(8)	0.013(8)
H313	0.6791(16)	0.6190(11)	-0.0187(13)	0.079(10)	0.029(7)	0.075(12)	0.028(7)	0.001(9)	0.019(8)
O32	0.7395(6)	0.5458(5)	0.2593(4)	0.035(3)	0.014(3)	0.010(3)	0.000(3)	-0.001(2)	-0.003(2)
C32	0.6173(6)	0.5239(5)	0.2921(5)	0.036(3)	0.018(3)	0.029(3)	0.006(3)	0.019(3)	0.005(3)
H321	0.6180(13)	0.4505(10)	0.3308(12)	0.043(7)	0.030(8)	0.076(10)	0.016(5)	0.024(7)	0.023(7)
H322	0.5509(12)	0.5224(13)	0.2283(13)	0.030(6)	0.071(11)	0.083(11)	0.003(7)	0.010(7)	0.010(10)
H323	0.5907(16)	0.5805(13)	0.3453(13)	0.077(10)	0.046(9)	0.093(11)	0.003(8)	0.052(9)	-0.010(9)
O33	0.9260(6)	0.5355(6)	0.1708(6)	0.020(3)	0.020(3)	0.064(5)	-0.009(3)	-0.003(3)	0.011(4)
C33	1.0454(6)	0.4904(7)	0.1801(7)	0.009(3)	0.044(5)	0.079(5)	-0.005(3)	-0.012(3)	0.011(5)
H331	1.0480(14)	0.4177(17)	0.1602(22)	0.023(7)	0.066(13)	0.221(28)	0.007(8)	-0.020(10)	-0.052(15)
H332	1.1056(20)	0.5356(20)	0.1472(29)	0.050(10)	0.100(18)	0.279(40)	-0.025(13)	0.048(18)	0.041(23)
H333	1.0735(26)	0.4879(26)	0.2530(24)	0.107(19)	0.163(28)	0.151(24)	0.074(19)	-0.068(18)	0.021(22)
P4	0.8233(5)	0.2757(5)	0.0494(5)	0.009(3)	0.013(3)	0.023(3)	0.001(3)	0.007(2)	-0.002(3)
O41	0.9261(5)	0.3410(5)	-0.0040(4)	0.014(3)	0.024(3)	0.025(3)	-0.002(2)	0.008(2)	0.008(3)
C41	0.9700(6)	0.3203(5)	-0.0985(4)	0.027(3)	0.024(3)	0.024(3)	0.001(3)	0.010(3)	0.008(3)
H411	1.0445(14)	0.3681(12)	-0.1168(10)	0.060(8)	0.056(9)	0.041(7)	-0.028(8)	0.027(6)	-0.002(6)
H412	0.8984(13)	0.3324(14)	-0.1533(11)	0.039(7)	0.098(13)	0.046(8)	0.017(8)	0.011(6)	0.014(8)
H413	0.9996(14)	0.2452(10)	-0.1054(10)	0.064(8)	0.030(8)	0.048(7)	0.008(6)	0.022(6)	0.006(6)
O42	0.8751(5)	0.1637(4)	0.0273(4)	0.017(3)	0.012(3)	0.026(3)	0.007(2)	-0.002(2)	0.002(2)
C42	0.9880(5)	0.1348(4)	0.0750(5)	0.015(3)	0.017(3)	0.030(3)	0.008(2)	0.001(2)	0.006(3)
H421	0.9795(12)	0.1410(13)	0.1548(13)	0.035(6)	0.070(10)	0.068(11)	0.002(7)	-0.004(7)	-0.010(9)
H422	1.0067(12)	0.0594(9)	0.0522(11)	0.046(7)	0.021(7)	0.090(10)	0.024(5)	-0.033(7)	-0.019(7)
H423	1.0632(10)	0.1823(11)	0.0538(10)	0.012(5)	0.070(9)	0.065(8)	-0.011(6)	-0.007(5)	0.019(8)
O43	0.7151(5)	0.2711(5)	-0.0315(4)	0.016(3)	0.029(3)	0.024(3)	0.005(3)	0.005(2)	-0.005(3)
C43	0.5966(5)	0.3148(5)	-0.0167(4)	0.008(2)	0.026(3)	0.032(3)	0.002(2)	-0.004(2)	-0.001(3)
H431	0.5931(11)	0.3353(16)	0.0645(11)	0.029(6)	0.143(17)	0.048(8)	-0.004(8)	0.021(6)	-0.046(10)
H432	0.5259(13)	0.2604(12)	-0.0310(14)	0.033(7)	0.058(9)	0.128(14)	-0.020(7)	0.000(7)	-0.054(10)
H433	0.5827(14)	0.3788(12)	-0.0604(15)	0.045(8)	0.046(9)	0.106(13)	0.025(7)	0.008(8)	0.010(10)
P5	0.6800(5)	0.0099(5)	0.1891(5)	0.012(3)	0.012(3)	0.020(3)	0.001(2)	-0.002(2)	0.004(3)
O51	0.8267(5)	-0.0178(5)	0.1903(5)	0.013(2)	0.024(3)	0.033(3)	0.005(2)	0.005(2)	-0.002(3)
C51	0.8961(5)	-0.0081(5)	0.2818(4)	0.016(3)	0.022(3)	0.023(3)	0.002(2)	-0.005(2)	-0.002(3)
H511	0.8923(13)	0.0680(11)	0.3077(11)	0.051(7)	0.031(8)	0.065(8)	0.018(6)	-0.015(6)	0.009(7)
H512	0.8587(13)	-0.0588(10)	0.3360(11)	0.056(8)	0.029(7)	0.050(8)	0.002(6)	0.001(6)	0.002(6)
H513	0.9907(11)	-0.0275(12)	0.2669(10)	0.017(5)	0.072(10)	0.063(8)	0.007(6)	-0.008(5)	-0.024(8)
O52	0.6485(6)	-0.0299(5)	0.0793(5)	0.025(3)	0.020(3)	0.030(3)	0.008(3)	-0.004(2)	-0.008(3)
C52	0.6112(6)	0.0371(6)	0.0030(4)	0.033(3)	0.033(4)	0.022(3)	-0.013(3)	-0.001(3)	0.003(3)
H521	0.5751(16)	0.1008(12)	0.0309(9)	0.097(11)	0.045(8)	0.020(6)	0.021(8)	-0.021(6)	0.018(7)
H522	0.5455(17)	0.0012(13)	-0.0461(12)	0.079(10)	0.054(9)	0.070(10)	-0.010(9)	-0.023(9)	0.023(9)
H523	0.6920(16)	0.0545(19)	-0.0418(12)	0.059(9)	0.152(20)	0.054(8)	-0.043(11)	0.019(8)	-0.010(11)
O53	0.6286(6)	-0.0826(4)	0.2536(4)	0.019(3)	0.014(3)	0.025(3)	0.000(2)	0.004(2)	0.003(3)
C53	0.6610(6)	-0.1839(5)	0.2285(5)	0.026(3)	0.010(3)	0.042(3)	-0.001(3)	-0.006(3)	-0.005(3)
H531	0.6292(23)	-0.2323(13)	0.2824(19)	0.144(18)	0.028(8)	0.141(18)	-0.018(10)	0.081(16)	-0.021(11)
H532	0.6196(19)	-0.2003(10)	0.1564(14)	0.122(14)	0.025(7)	0.109(13)	0.027(8)	-0.081(12)	-0.038(8)
H533	0.7567(17)	-0.1912(12)	0.2217(17)	0.049(9)	0.043(9)	0.151(17)	0.013(7)	0.009(9)	-0.027(11)
P6	0.4363(6)	0.1214(5)	0.2634(4)	0.016(3)	0.015(3)	0.013(3)	-0.003(2)	0.003(2)	-0.004(3)
O61	0.3740(5)	0.0842(5)	0.3628(4)	0.010(2)	0.027(3)	0.019(3)	-0.003(2)	0.001(2)	-0.005(3)
C61	0.4275(5)	0.0005(5)	0.4135(4)	0.023(3)	0.028(3)	0.022(3)	-0.005(2)	0.001(2)	0.003(3)
H611	0.5240(16)	0.0011(16)	0.4071(14)	0.053(9)	0.101(14)	0.103(13)	0.035(9)	0.030(9)	0.070(12)
H612	0.4014(22)	0.0138(20)	0.4869(13)	0.128(16)	0.138(21)	0.043(9)	0.013(15)	0.025(10)	0.023(12)
H613	0.3981(26)	-0.0669(12)	0.3844(17)	0.179(22)	0.020(8)	0.131(18)	0.000(10)	-0.095(17)	0.029(10)
O62	0.3830(5)	0.0430(4)	0.1830(4)	0.008(2)	0.017(3)	0.030(3)	-0.007(2)	-0.005(2)	-0.009(3)
C62	0.2571(5)	0.0091(5)	0.1863(5)	0.008(2)	0.033(4)	0.032(3)	-0.005(3)	-0.004(2)	-0.005(3)
H621	0.2347(12)	-0.0243(13)	0.1133(13)	0.034(6)	0.085(12)	0.094(12)	-0.039(7)	0.020(7)	-0.053(10)
H622	0.2471(11)	-0.0460(10)	0.2450(11)	0.028(6)	0.045(8)	0.067(9)	-0.025(5)	0.005(6)	0.010(8)
H623	0.1935(12)	0.0694(12)	0.1994(11)	0.032(6)	0.056(9)	0.072(9)	0.008(7)	0.003(6)	-0.007(8)
O63	0.3426(5)	0.2142(5)	0.2494(5)	0.012(2)	0.023(3)	0.038(3)	0.004(2)	0.003(2)	-0.003(3)
C63	0.3699(6)	0.2950(5)	0.1878(5)	0.019(3)	0.028(4)	0.045(4)	0.005(3)	0.009(3)	0.017(3)
H631	0.4677(13)	0.3186(15)	0.1945(14)	0.027(7)	0.080(11)	0.123(14)	-0.004(7)	0.007(8)	0.031(11)
H632	0.3131(20)	0.3552(15)	0.2082(21)	0.092(13)	0.060(11)	0.187(23)	0.042(11)	0.063(14)	0.085(14)
H633	0.3543(19)	0.2687(17)	0.1117(16)	0.091(13)	0.096(15)	0.079(13)	-0.042(12)	-0.026(10)	0.002(12)

[a] Thermal parameters correspond to the expression $T = -[2\pi^2(U_{11}h^2a^{*2} + \ldots + 2U_{12}hka^*b^* + \ldots)]$. Estimated standard deviations are in parentheses.

appear that the Rh(1)–H(1)–Rh(3) bond is significantly asymmetric whereas Rh(1)–H(2)–Rh(2), which lies nearly in the Rh_3 plane, is symmetric. The asymmetry of the Rh–H–Rh bond centered at H(3) is intermediate between those at H(1) and H(2). It is interesting to note that the degree of asymmetry of the hydride environments as reflected by the H–P nonbonded separations (see Figure 1) follows the same pattern (H(1)–P(2) = 2.97 (1) Å vs. H(1)–P(6) = 2.68 (1) Å, H(2)–P(1) = H(2)–P(3) = 2.53 Å, and H(3)–P(4) = 2.90 (1) Å vs. H(3)–P(5) = 2.80 (1) Å).

Table II. Bond Distances (Å) and Angles (Deg) for $\{HRh[P(OCH_3)_3]_2\}_3$[a]

Distances

Rh(1)-Rh(2)	2.803 (7)	P(5)-O(51)	1.626 (8)	C(11)-H(113)	1.04 (2)	C(41)-H(412)	1.06 (2)
Rh(1)-Rh(3)	2.780 (6)	P(5)-O(52)	1.597 (9)	C(12)-H(121)	1.04 (2)	C(41)-H(413)	1.06 (2)
Rh(2)-Rh(3)	2.855 (7)	P(5)-O(53)	1.623 (8)	C(12)-H(122)	1.03 (2)	C(42)-H(421)	1.08 (2)
Rh(1)-H(1)	1.838 (10)	P(6)-O(61)	1.593 (8)	C(12)-H(123)	1.06 (2)	C(42)-H(422)	1.08 (1)
Rh(1)-H(2)	1.734 (11)	P(6)-O(62)	1.604 (8)	C(13)-H(131)	1.12 (2)	C(42)-H(423)	1.08 (2)
Rh(2)-H(2)	1.732 (11)	P(6)-O(63)	1.614 (9)	C(13)-H(132)	1.08 (2)	C(43)-H(431)	1.13 (2)
Rh(2)-H(3)	1.753 (13)	O(11)-C(11)	1.428 (9)	C(13)-H(133)	1.11 (1)	C(43)-H(432)	1.07 (1)
Rh(3)-H(1)	1.750 (12)	O(12)-C(12)	1.417 (8)	C(21)-H(211)	1.04 (2)	C(43)-H(433)	1.05 (2)
Rh(3)-H(3)	1.785 (12)	O(13)-C(13)	1.434 (9)	C(21)-H(212)	1.03 (2)	C(51)-H(511)	1.08 (2)
Rh(1)-P(1)	2.155 (7)	O(21)-C(21)	1.418 (9)	C(21)-H(213)	0.98 (3)	C(51)-H(512)	1.08 (2)
Rh(1)-P(2)	2.197 (8)	O(22)-C(22)	1.421 (9)	C(22)-H(221)	1.07 (2)	C(51)-H(513)	1.08 (1)
Rh(2)-P(3)	2.164 (9)	O(23)-C(23)	1.404 (9)	C(22)-H(222)	1.06 (2)	C(52)-H(521)	1.02 (2)
Rh(2)-P(4)	2.202 (8)	O(31)-C(31)	1.439 (9)	C(22)-H(223)	1.05 (2)	C(52)-H(522)	1.07 (2)
Rh(3)-P(5)-	2.178 (9)	O(32)-C(32)	1.434 (9)	C(23)-H(231)	1.03 (2)	C(52)-H(523)	1.10 (2)
Rh(3)-P(6)	2.180 (8)	O(33)-C(33)	1.425 (10)	C(23)-H(232)	0.96 (3)	C(53)-H(531)	1.04 (3)
P(1)-O(11)	1.623 (8)	O(41)-C(41)	1.396 (8)	C(23)-H(233)	1.18 (2)	C(53)-H(532)	1.08 (2)
P(1)-O(12)	1.603 (9)	O(42)-C(42)	1.415 (8)	C(31)-H(311)	1.03 (2)	C(53)-H(533)	1.04 (2)
P(1)-O(13)	1.611 (9)	O(43)-C(43)	1.426 (8)	C(31)-H(312)	1.07 (2)	C(61)-H(611)	1.05 (2)
P(2)-O(21)	1.601 (8)	O(51)-C(51)	1.428 (8)	C(31)-H(313)	1.09 (2)	C(61)-H(612)	1.05 (2)
P(2)-O(22)	1.619 (8)	O(52)-C(52)	1.414 (9)	C(32)-H(321)	1.111 (1)	C(61)-H(613)	1.03 (2)
P(2)-O(23)	1.593 (9)	O(53)-C(53)	1.447 (9)	C(32)-H(322)	1.10 (2)	C(62)-H(621)	1.10 (2)
P(3)-O(31)	1.626 (9)	O(61)-C(61)	1.429 (9)	C(32)-H(323)	1.09 (2)	C(62)-H(622)	1.09 (2)
P(3)-O(32)	1.607 (8)	O(62)-C(62)	1.435 (8)	C(33)-H(331)	1.01 (3)	C(62)-H(623)	1.08 (2)
P(3)-O(33)	1.601 (9)	O(63)-C(63)	1.400 (9)	C(33)-H(332)	1.00 (3)	C(63)-H(631)	1.10 (2)
P(4)-O(41)	1.601 (8)	C(11)-H(111)	1.04 (2)	C(33)-H(333)	1.02 (3)	C(63)-H(632)	1.06 (2)
P(4)-O(42)	1.636 (8)	C(11)-H(112)	1.12 (2)	C(41)-H(411)	1.06 (2)	C(63)-H(633)	1.09 (2)
P(4)-O(43)	1.573 (9)						

Angles

Rh(1)-Rh(2)-Rh(3)	58.8 (2)	H(1)-Rh(3)-P(5)	171.7 (5)	Rh(3)-P(6)-O(63)	116.8 (4)	P(1)-O(11)-C(11)	120.7 (6)
Rh(2)-Rh(3)-Rh(1)	59.6 (2)	H(1)-Rh(3)-P(6)	85.4 (4)	O(11)-P(1)-O(12)	102.4 (5)	P(1)-O(12)-C(12)	123.2 (6)
Rh(3)-Rh(1)-Rh(2)	61.5 (2)	Rh(1)-P(1)-O(11)	118.3 (4)	O(11)-P(1)-O(13)	96.9 (5)	P(1)-O(13)-C(13)	117.3 (5)
H(1)-Rh(1)-H(2)	91.9 (5)	Rh(1)-P(1)-O(12)	115.6 (4)	O(12)-P(1)-O(13)	99.7 (5)	P(2)-O(21)-C(21)	122.2 (6)
H(2)-Rh(2)-H(3)	92.5 (6)	Rh(1)-P(1)-O(13)	120.4 (4)	O(21)-P(21)-O(22)	102.5 (5)	P(2)-O(22)-C(22)	121.5 (5)
H(1)-Rh(3)-H(3)	90.8 (6)	Rh(1)-P(2)-O(21)	111.7 (4)	O(21)-P(2)-O(23)	103.2 (5)	P(2)-O(23)-C(23)	122.9 (6)
P(1)-Rh(1)-P(2)	91.3 (3)	Rh(1)-P(2)-O(22)	119.3 (4)	O(22)-P(2)-O(23)	93.6 (5)	P(3)-O(31)-C(31)	120.4 (5)
P(3)-Rh(2)-P(4)	93.9 (3)	Rh(1)-P(2)-O(23)	123.2 (4)	O(31)-P(3)-O(32)	100.1 (4)	P(3)-O(32)-C(32)	118.6 (5)
P(5)-Rh(3)-P(6)	94.9 (3)	Rh(2)-P(3)-O(31)	114.9 (4)	O(31)-P(3)-O(33)	99.9 (5)	P(3)-O(33)-C(33)	122.4 (6)
H(1)-Rh(1)-P(1)	171.7 (4)	Rh(2)-P(3)-O(32)	118.3 (4)	O(32)-P(3)-O(33)	95.3 (5)	P(4)-O(41)-C(41)	123.8 (6)
H(1)-Rh(1)-P(2)	94.2 (4)	Rh(2)-P(3)-O(33)	123.9 (4)	O(41)-P(4)-O(42)	100.3 (4)	P(4)-O(42)-C(42)	117.7 (5)
H(2)-Rh(1)-P(1)	80.9 (4)	Rh(2)-P(4)-O(41)	114.7 (4)	O(41)-P(4)-O(43)	102.8 (5)	P(4)-O(43)-C(43)	122.6 (5)
H(2)-Rh(1)-P(2)	160.1 (4)	Rh(2)-P(4)-O(42)	116.7 (4)	O(42)-P(4)-O(43)	95.1 (5)	P(5)-O(51)-C(51)	118.3 (5)
H(2)-Rh(2)-P(3)	79.8 (4)	Rh(2)-P(4)-O(43)	123.3 (4)	O(51)-P(5)-O(52)	96.5 (5)	P(5)-O(52)-C(52)	120.4 (6)
H(2)-Rh(2)-P(4)	166.3 (5)	Rh(3)-P(5)-O(51)	115.8 (4)	O(51)-P(5)-O(53)	99.6 (5)	P(5)-O(53)-C(53)	120.5 (5)
H(3)-Rh(2)-P(3)	172.3 (6)	Rh(3)-P(5)-O(52)	128.1 (4)	O(52)-P(5)-O(53)	99.8 (5)	P(6)-O(61)-C(61)	118.2 (5)
H(3)-Rh(2)-P(4)	93.6 (5)	Rh(3)-P(5)-O(53)	112.4 (4)	O(61)-P(6)-O(62)	101.9 (5)	P(6)-O(62)-C(62)	120.6 (5)
H(3)-Rh(3)-P(5)	89.1 (5)	Rh(3)-P(6)-O(61)	123.3 (4)	O(61)-P(6)-O(63)	93.6 (5)	P(6)-O(63)-C(63)	121.7 (5)
H(3)-Rh(3)-P(6)	175.5 (5)	Rh(3)-P(6)-O(62)	114.9 (4)	O(62)-P(6)-O(63)	102.6 (5)		

[a] The estimated standard deviations in parentheses for this and the subsequent table refer to the least significant figure.

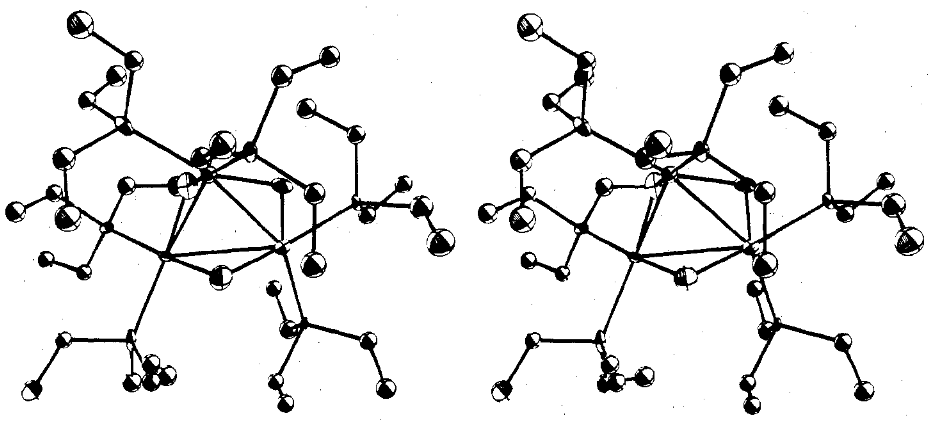

Figure 2. Stereoscopic drawing of $\{HRh[P(OCH_3)_3]_2\}_3$ as derived from neutron diffraction data (T = 110 K) with methoxy hydrogen atoms eliminated for clarity. Thermal ellipsoids are scaled to enclose 50% probability.

As a result of the unusual arrangement of the $\{HRhP_2\}_3$ cluster core, the average distance of a hydride ligand from the Rh–Rh vector which it spans is ~1.1 Å. If the hydride ligands were located closer to the Rh–Rh vectors, they in fact would lie closer to the projections of the Rh–P vectors. Actual trans P–Rh–H angles range from 160.1 (4) to 175.5 (5)°. Since the projections of most of the Rh–P vectors pass closer to the Rh–Rh vectors than do the hydride ligands, the M–H–M interactions here closely resemble the "closed" and bent (3c-2e) M–H–M type of interaction.

Table III. Intermolecular Nonbonded Interactions with Distances Less Than 2.5 Å

$H(131) \rightarrow H(113)^a = 2.20\ (2)$
$H(132) \rightarrow H(231)^a = 2.39\ (3)$
$O(21) \rightarrow H(613)^b = 2.473\ (7)$
$H(221) \rightarrow H(611)^b = 2.35\ (1)$
$H(221) \rightarrow H(531)^b = 2.40\ (1)$
$H(311) \rightarrow H(532)^c = 2.30\ (1)$
$H(312) \rightarrow H(423)^d = 2.38\ (2)$
$H(313) \rightarrow H(633)^e = 2.39\ (1)$
$H(313) \rightarrow H(621)^e = 2.50\ (2)$
$H(322) \rightarrow H(612)^b = 2.43\ (2)$
$H(411) \rightarrow H(513)^d = 2.48\ (2)$
$H(411) \rightarrow O(51)^d = 2.31\ (1)$
$H(412) \rightarrow H(621)^e = 2.47\ (2)$
$H(432) \rightarrow H(532)^e = 2.33\ (2)$
$H(433) \rightarrow H(621)^e = 2.48\ (2)$

$^a\ 2-X, {}^1/_2+Y, 1-Z.$ $^b\ 1-X, {}^1/_2+Y, 1-Z.$ $^c\ X, Y+1, Z.$ $^d\ 2-X, {}^1/_2+Y, -Z.$ $^e\ 1-X, {}^1/_2+Y, -Z.$

It is interesting to consider the structural and electronic effects of hypothetically constraining the three pseudo-square-planar H_2RhP_2 moieties to lie in the Rh_3 plane with the Rh–Rh and Rh–H distances fixed at the experimental values. As demonstrated elswhere the M–H–M linkage is flexible and easily deformed.[21] The result of this constraint would be to increase the M–H–M angle from an average value of about 106° to 150°. This would decrease the average hydrogen to Rh–Rh vector separation to about 0.38 Å. Imposition of the D_{3h} symmetry constraint would cause the Rh–Rh (predominantly) antibonding orbitals to acquire two electrons from the Rh–Rh bonds which is energetically unfavorable for the formation of a cyclic Rh_3 system. (Professor J. Fackler pointed out to us some time ago that consideration of the second-order terms in the Jahn–Teller theorem predicts for $\{HRh[P(OCH_3)_3]_2\}_3$ a stabilization upon distortion from D_{3h} symmetry.) Interestingly, while this constraint greatly increases the linearity of the M–H–M system, it only slightly increases the steric interactions of the phosphite ligands. The average nonbonded P···P contacts on adjacent metal atoms decrease slightly from 4.36 (4) to ca. 4.0 Å. If the experimental H–Rh–P angles are maintained, the decrease becomes negligible. This analysis leads to the conclusion that the basic geometry of the $\{HRhP_2\}_3$ cluster core is determined predominantly by electronic and not by steric factors. A critical test of this hypothesis would be the structural characterization of an analogous $\{HRhP_2\}_3$ cluster containing phosphite ligands less bulky than $P(OCH_3)_3$ groups, to determine if the present geometry is indeed retained.

Efforts are also presently under way to synthesize larger oligomers of the $\{HRhP_2\}_x$ series. In view of the apparently preferred pseudo-square-planar geometry of the H_2RhP_2 unit, and the observed configuration of **2**, it is likely that $\{HRhP_2\}_x$ oligomers with $x > 3$ will also possess cyclic structures. Possible structural models for a tetramer are displayed in Figure 3. Configurations 3-I and 3-III are limiting extremes of the same structure which can be infinitely varied between the tetrahedral form 3-I and the planar form 3-III. Variation of the tetrameric structure is accomplished by elongation of the "butterfly" vectors (Rh(2) → Rh(4) and Rh(1) → Rh(3)). The tetrameric structure 3-I comprises two coplanar H_2RhP_2 units centered at Rh(2) and Rh(4) which are normal to those centered at Rh(1) and Rh(3). Elongation of the "butterfly" vectors and concomitant bending of the Rh–H–Rh angle, in addition to bending of the H_2RhP_2 dihedral angles, will eventually lead to the completely planar structure 3-III. The degree of distortion between 3-I and 3-III will depend on the electronic and steric requirements of the Rh_4 tetramer and the size of the coordinated phosphite ligands. An analogous situation can be envisioned for the hexameric complex as displayed in Figure 4. Although the polygonal bases for these proposed structures are tetrahedral and octahedral arrays of Rh atoms, the cyclic nature is readily apparent.

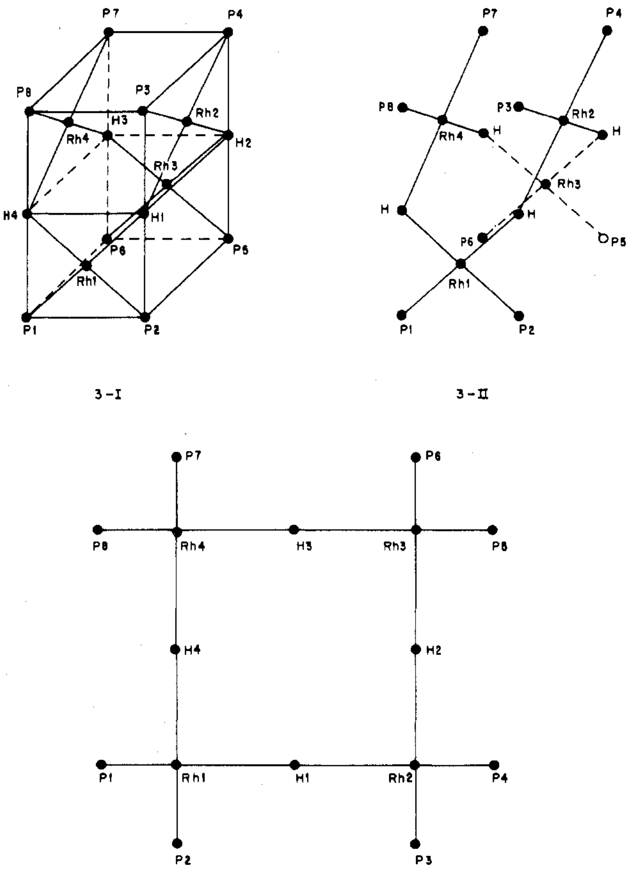

3-I 3-II

3-III

Figure 3. Probable structural models for a tetrameric $H_4Rh_4P_8$ oligomer. The cyclic nature and variability of configurations are readily apparent.

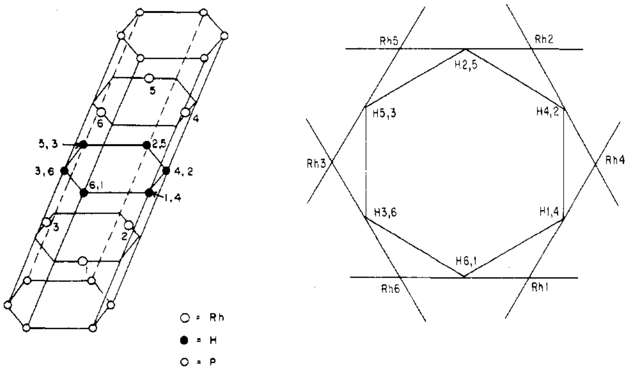

4-I 4-II

Figure 4. Structural model for a cyclic $H_6Rh_6P_{12}$ hexamer. Conversion from 4-I to 4-II is accomplished by folding the Rh–H(2) triangles along the H–H vector.

Registry No. 2, 65176-61-6.

Supplementary Material Available: A listing of structure factor amplitudes (16 pages). Ordering information is given on any current masthead page.

---

[21] (a) Bau, R.; Koetzle, T. F. *Pure Appl. Chem.* **1978**, 50, 54. (b) Bau, R.; Teller, R. G.; Kirtley, S. W. *Acc. Chem. Res.* **1979**, 12, 176.